Effect of Organoclays on the Properties of Polyurethane/Clay Nanocomposite Coatings

Hua Jin, Jeong Jae Wie, Sung Chul Kim

Polymer Engineering Laboratory, Department of Chemical and Biomolecular Engineering, Korea Advanced Institute of Science and Technology, 373-1 Guseong-Dong, Yuseong-Gu, Daejeon 305-701, South Korea

Received 16 April 2009; accepted 29 June 2009
DOI 10.1002/app.31040
Published online 7 April 2010 in Wiley InterScience (www.interscience.wiley.com).

ABSTRACT: Linear, one-binding-site or two-binding-site (N^+) organifiers with two hydroxyl end groups were synthesized, and novel organoclays were prepared through a cation-exchange reaction between pristine sodium montmorillonite and the synthesized organifiers. After sonication of the as-prepared organoclay in *N*,*N*′-dimethylformamide for 10 min, the average size of the clay decreased to about 1 μm. The X-ray diffraction patterns confirmed that the *d*-spacing of the silicate layers of the organoclay expanded from 1.1 to about 1.9 nm and the peak intensity decreased with the molecular weight of the organifier increasing. Polyurethane/clay nanocomposites were synthesized by a one-shot polymerization method. Both intercalated and exfoliated structures of the layered silicates in the polyurethane matrix were observed from transmission electron microscopy micrographs, and the *d*-spacing ranged from 4 to 10 nm. The thermal and mechanical properties of the nanocomposite were enhanced by the introduction of the organoclay into the polyurethane matrix. An approximately 40–46°C increase in the onset decomposition temperature, a 200% increase in the tensile strength with a 0.5 wt % clay loading, and a 49% increase in Young's modulus with a 3 wt % clay loading were achieved. The effects of the molecular weight and the number of binding sites of the organifier on the properties of the nanocomposites were also evaluated. J Appl Polym Sci 117: 2090–2100, 2010

Key words: nanocomposites; organoclay; polyurethanes; nanocomposites

INTRODUCTION

The use of nanoclays to enhance the thermal, physical, and mechanical properties of polymers at low clay loadings has attracted interest from industry and academia and has flourished for 20 years.[1,2] Montmorillonite (MMT) is one of the most promising layered silicate clays used as an inorganic filler because of its high in-plane strength, stiffness, high aspect ratio, and natural abundance. Additionally, the Na^+, K^+, or Ca^+ ions residing in the interlayer galleries can be replaced by organic cations such as alkylammonium via a cation-exchange reaction; this makes the silicate layer organophilic and compatible with the polymer matrices. Moreover, the interfacial interaction between the polymer and the silicate layer is enhanced by the introduction of the organic compound if the organifier has reactive functional groups to become part of the polymer chain.[3]

The first study of polymer/clay nanocomposites was pioneered by the Toyota research group.[2,4–6] Since then, extensive studies of polymer/clay nanocomposites based on polymers such as polycaprolactone,[7,8] polystyrene,[9–11] polyimide,[12,13] polylactide,[14,15] polypropylene,[16–18] poly(vinylidene fluoride),[19] and poly(methyl methacrylate)[20–22] have been undertaken to obtain new organic–inorganic nanocomposites with enhanced properties.

Polyurethanes (PUs) are known as very useful materials in industrial applications such as coatings, adhesives, foams, fibers, and thermoplastic elastomers because their properties can be tailored by simple adjustments of the compositions or the processing conditions. Since the first PU/clay nanocomposite with greatly improved properties was reported by Wang and Pinnavaia,[23] several PU/clay nanocomposites have been studied by different groups.[3,24–46] To improve both the thermal stability and mechanical properties of PUs, which are associated with the morphology and dispersion efficiency of the organoclay particles in the polymer matrix, there have been attempts to prepare organoclays with different organifiers (organomodifiers of the layered silicate) containing reactive end groups that can react with isocyanate groups in the formation of PU/organoclay nanocomposites[3,26–30,39,40] or with the addition of hyperbranched polymers to PU to help with the exfoliation of nanocomposites without aggregation.[24]

To the best of our knowledge, no information has been presented about synthesizing organoclays with multibinding-site organifiers with urethane groups

Correspondence to: S. C. Kim (kimsc@kaist.ac.kr).

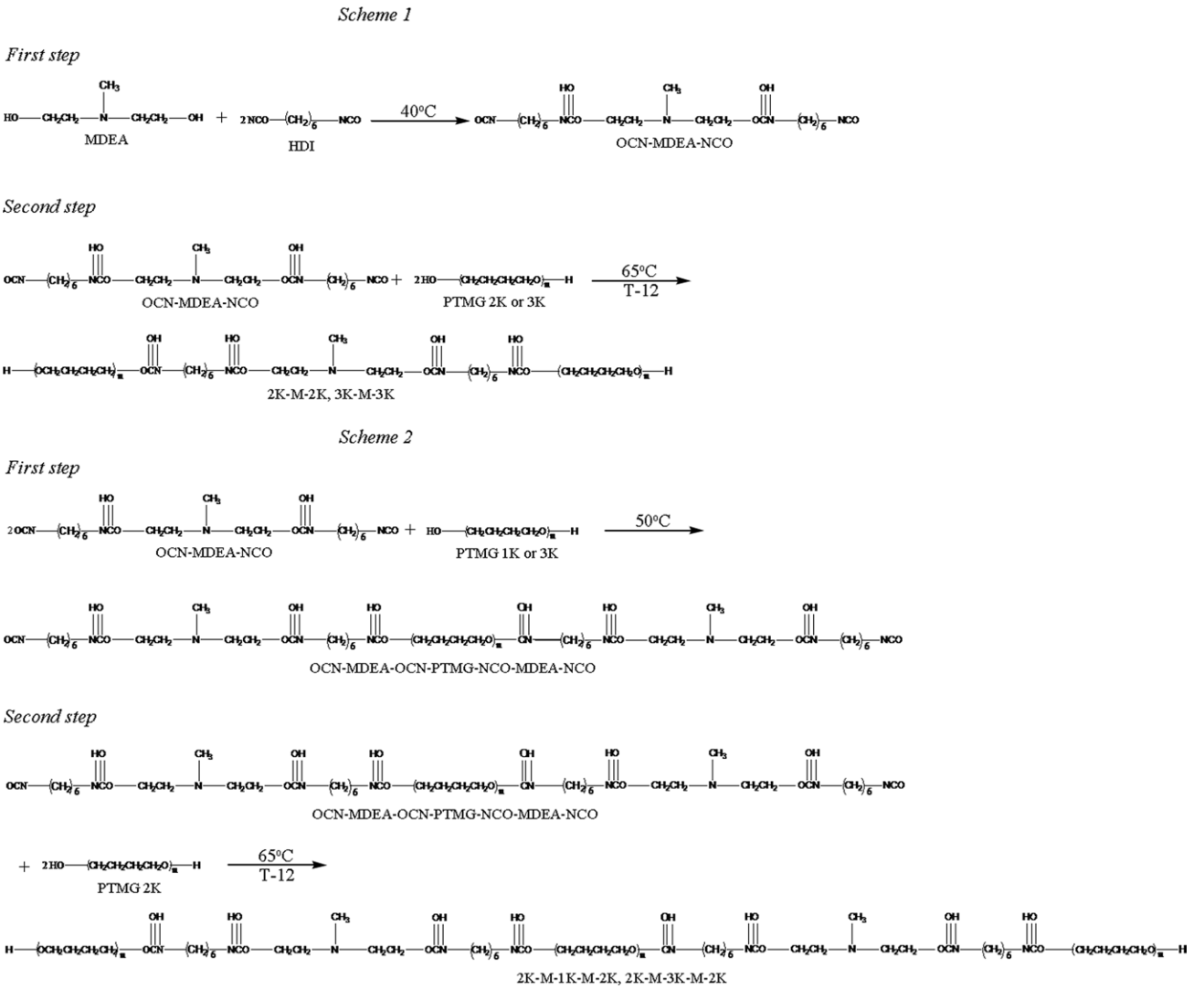

Figure 1 Reaction schemes for the synthesis of organifiers.

and hydroxyl end groups to enhance compatibility with PU and to react with isocyanate. Our goal in this study was to prepare an organoclay using organifiers with different molecular weights and multiple cation sites to enlarge the *d*-spacing of the clay and with two hydroxyl end groups to react with isocyanate during *in situ* polymerization. In addition, the effects of the various organoclays on the morphology and thermal and mechanical properties of PU/clay nanocomposites were investigated.

EXPERIMENTAL

Materials

MMT (Cloisite Na^+, Southern Clay Product, Inc., Gonzales, TX) with a cation-exchange capacity of 92.6 mequiv/100 g was dried at 80°C for 24 h *in vacuo* before use. *N*-Methyl diethanol amine (MDEA; Aldrich Chemical Co., Inc.; 99%, Yongin, Korea) and poly(tetramethylene ether glycol) (PTMG) with a number-average molecular weight of 1000 (PTMG1K), 2000 (PTMG2K), or 2900 (PTMG3K; Korea PTG Co., Ltd., Seoul, Korea) were degassed overnight at 80°C *in vacuo* to remove moisture before use. Hexamethylene diisocyanate (Tokyo Kasei Kogyo Co., Ltd.; 98%, Tokyo, Japan) was used as received. Poly(ethylene adipate)diol (PEA; number-average molecular weight = 2000; Kunsul Chemical Industrial Co., Ltd., Seoul, Korea) and 1,4-butanediol (1,4-BD; Aldrich Chemical; 99%, Yongin, Korea) were degassed overnight at 80°C and at room temperature, respectively, to remove moisture before use. *N,N′*-Dimethylformamide (DMF; Merck GmbH, Darmstadt, Germany; 99.8%) was stored over 4-Å molecular sieves. 4,4′-Dipheylmethane diisocyanate (MDI; Tokyo Kasei Kogyo; 98%, Tokyo, Japan) and dibutyltin dilaurate(T-12; Aldrich Chemical, Yongin, Korea) were used as received.

Preparation of the organifiers

Two kinds of chain-extended organifiers with urethane groups, that is, linear one-binding-site and

linear two-binding-site organifiers, were synthesized as shown in Figure 1. For the linear one-binding-site (N^+) organifier (Scheme 1 in Fig. 1), isocyanate-terminated MDEA (OCN–MDEA–NCO) was prepared by the reaction of 2 equiv of hexamethylene diisocyanate with 1 equiv of MDEA first. The reaction was carried out at 40°C until the theoretical isocyanate content (as determined by the di-*n*-butylamine titration method[47]) was reached. Then, the organifier was synthesized by the dropping of 1 equiv of OCN–MDEA–NCO into 2 equiv of PTMG2K or PTMG3K at 65°C. T-12 (0.05 wt %) was used as the catalyst. The reaction was terminated when the peak of the isocyanate group disappeared in the Fourier transform infrared (FTIR) measurement. For the two-binding-site organifier (Scheme 2 in Fig. 1), 1 equiv of PTMG1K or PTMG3K was dropped into 2 equiv of OCN–MDEA–NCO at 50°C, and then 1 equiv of the as-prepared product was dropped into 2 equiv of PTMG2K at 65°C. All the reactions were carried out under a nitrogen atmosphere. The organifiers in this study were coded as 2K-M-2K, 3K-M-3K, 2K-M-1K-M-2K, and 2K-M-3K-M-2K. Here, 1K, 2K, and 3K indicate the molecular weight of PTMG, and M indicates MDEA containing a quaternary ammonium binding site (N^+).

Preparation of the organoclays

To increase the compatibility or interaction between the hydrophobic PU and the hydrophilic clay and to increase the interlayer spacing of the clay, a cation-exchange reaction was performed between the pristine sodium montmorillonite (Na-MMT) and the organifier. The organoclay preparation method was as follows. A calculated amount of the organifier was dissolved in a mixture of isopropyl alcohol (IPA) and deionized water (IPA/water = 7:1 v/v) at 65°C, and the excess concentrated HCl (HCl/organifier = 2:1 mol/mol) was dropped into the organifier solution to quaternize the amine group. Na-MMT was preliminarily dispersed in a mixture of IPA and deionized water (IPA/water = 6:4 v/v) at 65°C with a mechanical stirrer. The organifier solution was poured into the suspension of MMT, and the mixture was vigorously stirred with a mechanical stirrer for 24 h at 65°C. The organically modified MMT was precipitated and washed with water until no AgCl precipitate was formed when the silver nitrate solution was dropped into the washing liquid. The organoclay was freeze-dried for 3 days and ground to a proper size.

Synthesis of the PU/clay nanocomposite films

The PU/clay nanocomposites were synthesized by a one-shot process, as described in our previous work.[3] To improve the organoclay dispersion in the PU matrix, various amounts of organoclay (0.5, 1, and 3 wt % with respect to PU) in DMF (2 wt % based on DMF) were sonicated for 10 min with an ultrasonicator (HD2070, Bandelin, Germany). The organoclay dispersion was poured into a DMF solution of PEA and a 1,4-BD mixture, and the dispersion was stirred for 30 min. MDI and T-12 (0.02 wt % based on the reaction solution) were charged into the mixture. The equivalent weight ratio of the components was 2.625:1.0:1.5 for MDI, PEA, and 1,4-BD. Polymerization was carried out under a nitrogen atmosphere for 5 h at 65°C, and the final solid content of the mixture was adjusted to 20 wt % by the addition of fresh DMF. The PU/clay nanocomposite films were formed via the casting of solutions onto a glass plate followed by the removal of the solvent in an oven at 80°C overnight. Neat PU was prepared with the same procedure without the addition of organoclays.

Characterization

Wide-angle X-ray diffraction (WAXD) was conducted at the ambient temperature on a Rigaku D/MAX-RC diffractometer (Seoul, Korea) with a Cu Kα radiation source at a scan speed of 1°/min in the range of 1.2–10°. FTIR measurements were conducted on synthesized organifiers and clays with a Jasco 470-plus FTIR spectrometer (Tokyo, Japan). Thermogravimetric analysis was performed under a nitrogen atmosphere with a TA Instruments TGA Q500 (San Jose, CA) to measure the inorganic content of the organoclays and the thermal stability of the neat PU and PU/clay nanocomposites. The measurements were carried out with a heating rate of 20°C/min in the temperature range of 40–950°C under nitrogen. The ion-exchanged fraction was defined as the fraction of active sites on layered silicates reacted with organifiers by a cation-exchange reaction as follows:

$$\text{Ion-exchanged fraction} = \frac{\text{Organifer content in organoclay (mmol/100 g of clay)}}{\text{CEC of montmorillonite (mequiv/100 g of clay)}}$$

The glass-transition temperature was measured with a Rheometric Scientific DMTA IV (Piscataway, NJ). The measurements were made at a fixed frequency of 1 Hz with a heating rate of 5°C/min over a temperature range of −70 to 70°C in a rectangular tension/compression mode. The organoclay samples for scanning electron microscopy (SEM) study were prepared via the spin coating of a dispersion of the organoclay in DMF after sonication for 10 min. The

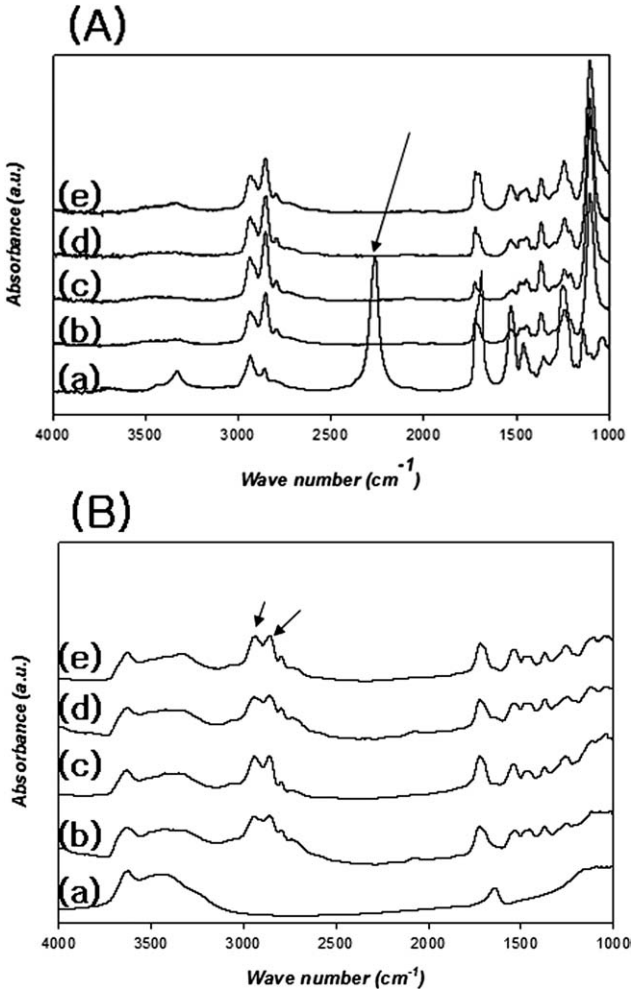

Figure 2 FTIR spectra of (A) organifiers [(a) OCN–MDEA–NCO, (b) 2K-M-2K organifier, (c) 3K-M-3K organifier, (d) 2K-M-1K-M-2K organifier, and (e) 2K-M-3K-M-2K organifier] and (B) clays [(a) Na-MMT, (b) 2K-M-2K organoclay, (c) 3K-M-3K organoclay, (d) 2K-M-1K-M-2K organoclay, and (e) 2K-M-3K-M-2K organoclay].

nanocomposite samples used to determine the clay dispersion in the PU matrix were prepared by the microtoming of a cross section of the nanocomposite first followed by plasma etching for 2 min. SEM images were obtained with a JEOL JSM-5610 SEM (Tokyo, Japan) after gold coating. Transmission electron microscopy (TEM) specimens for nanocomposites were prepared with an RMC MT-XL microtome (Tucson, AZ) with a cryogenic ultramicrotome system. The specimens were cut to be 50 nm thick with a diamond knife at −120°C. TEM micrographs were obtained with a Philips CM20 transmission electron microscope (Hillsboro, OR). The molecular weights of the polymer were measured with a Polymer Laboratories GPC 220 (Worcestershire, UK) system calibrated with polystyrene standards. The measurement temperature was 35°C, and tetrahydrofuran was used as the eluent. The pure PU was recovered from PU/clay nanocomposites with the following method. First, 0.2 g of the synthesized PU/clay nanocomposite was dissolved in 2 mL of DMF, and then the solution was poured into 20 mL of a 1% LiCl solution in DMF to perform the reverse ion-exchange reaction. After 48 h, the solution was centrifuged at 10,000 rpm for 2 min, and then the supernatant liquid was poured into the deionized water; the resulting solid was filtered and dried *in vacuo*. Tensile tests were carried out with an Instron 5583 (Norwood, MA) machine according to ASTM 638M. The specimen with 6 mm wide, a 25-mm grip distance was used, and the crosshead speed was set to 500 mm/min.

RESULTS AND DISCUSSION

Characterization of the organifiers and organoclays

The synthesis scheme for organifiers with the chemical structure is presented in Figure 1. Figure 2(A) shows the FTIR spectra of OCN–MDEA–NCO and organifiers. The peak for the isocyanate group (2272 cm^{-1}) disappeared after the reaction with PTMG. From these spectra, it was determined that an organifier with a urethane group had been successfully synthesized.

To determine the ion-exchanged fractions of the organoclays, thermogravimetric analysis was performed, and the results are listed in Table I. With the molecular weight of the organifier increasing, the inorganic content decreased to about 25% in the series (2K-M-2K and 3K-M-3K, 2K-M-1K-M-2K, and 2K-M-3K-M-2K). On the basis of the inorganic content of the organoclay and the molecular weight of the organifier, we could calculate the ion-exchanged

TABLE I
Properties of Na-MMT and Organoclays

	Residual weight percentage[a]	Molecular weight of the organifier	Ion-exchanged fraction	2θ (°)	*d*-spacing (nm)
Na-MMT	–	–	–	7.80	1.13
2K-M-2K	32.4	4400	0.51	4.60	1.92
3K-M-3K	24.4	6200	0.53	4.60	1.92
2K-M-1K-M-2K	43.0	5800	0.24	4.47	1.97
2K-M-3K-M-2K	32.4	7800	0.29	4.57	1.93

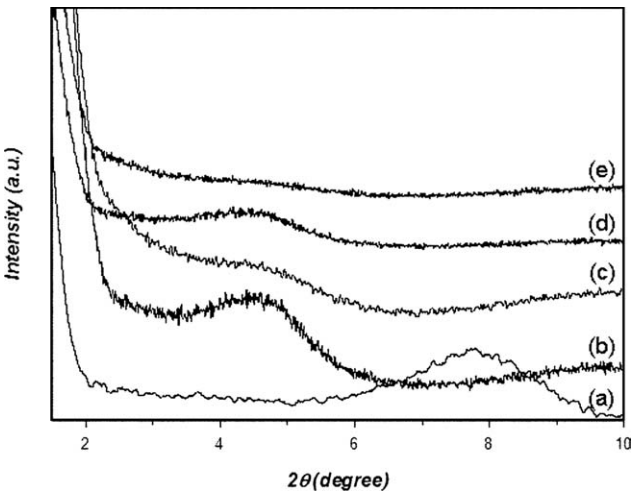

Figure 3 WAXD patterns of (a) Na-MMT, (b) 2K-M-2K organoclay, (c) 3K-M-3K organoclay, (d) 2K-M-1K-M-2K organoclay, and (e) 2K-M-3K-M-2K organoclay.

fraction of the organoclay, and the value was 0.51 for the 2K-M-2K organoclay; this means that 51% of the Na cations on the layered silicate were exchanged with the organifier via the cation-exchange reaction. However, the two-binding-site organoclays showed a somewhat lower value of the ion-exchanged fraction of approximately 0.25. We can learn from these results that the one-binding-site organifier more easily penetrated the silicate layers than the two-binding-site organifier, and there was some possibility that just one N^+ in the two-binding-site organifier was attached to the layered silicate surface. To confirm the successful modification of Na-MMT by the organifiers, FTIR was conducted [Fig. 2(B)]. All the spectra of the clays showed bands at 3636 and 3395 cm^{-1} due to O—H stretching for the silicate and water, respectively. Peaks at 1040 cm^{-1} were due to the stretching vibration of Si—O—Si from silicate. However, a new band appeared for the organoclays that did not exist for Cloisite Na^+. Bands at 2924, 2842, and 1475 cm^{-1} were attributed to C—H vibrations of methylene groups (asymmetric stretching, symmetric stretching, and bending, respectively). This demonstrates the successful cation exchange between the sodium cations and organifiers.

The X-ray diffraction (XRD) patterns of the synthesized organoclay are shown in Figure 3, and the corresponding data are given in Table I. The *d*-spacing of the pristine Na-MMT was 1.13 nm, whereas the *d*-spacing was increased to the maximum of 1.97 nm by the treatment with the reactive organifier [2K-M-1K-M-2K; Fig. 3(d)]. The *d*-spacings for the 2K-M-2K [Fig. 3(b)], 3K-M-3K [Fig. 3(c)], and 2K-M-3K-M-2K [Fig. 3(e)] organoclays were shown to be 1.92, 1.92, and 1.93 nm, respectively. It is worth noting that the molecular weight of the organifier affected the *d*-spacing of the resulting organoclay, and the peak intensity decreased with the molecular weight of the organifier increasing.

Figure 4 shows SEM images of the organoclays after sonication in DMF for 10 min. The average size of the organoclays decreased to about 1 μm after sonication, and this indicated that good dispersion of the organoclays in the PU matrix could be expected because of the small size. In addition, all the organoclays showed suspension stability in DMF because the organifier could be dissolved in DMF and act as a surfactant between the layered silicate and DMF.

Morphology

XRD patterns of the PU/clay nanocomposites are shown in Figure 5. No characteristic diffraction peaks appeared for the PU/clay nanocomposites with 0.5–3 wt % organoclay contents. The WAXD peaks of the layered silicates appeared only when there was uniform *d*-spacing between the silicates at certain orientations. No diffraction peaks for the PU/clay nanocomposites indicated that the *d*-spacing was greater than 3 nm, but these silicates were not necessarily exfoliated,[40] or the amount of clay was too small to be detected (3 wt % 2K-M-2K organoclay corresponded to an inorganic content of only 0.96 wt %). However, with the organoclay content increasing, there still existed some agglomeration of the clay, as shown in SEM images [Fig. 6(B,D)]. Small clay particles ranging from 5 to 10 μm were observed in 3 wt % organoclay loaded nanocomposites. In the case of nanocomposites containing 3 wt % organoclay [Fig. 7(B,D,F,H)], an intercalated morphology with nearly parallel layered silicates with a basal spacing ranging from 4 to 7 nm was observed as well as a small portion of exfoliated silicates. For the nanocomposites containing 0.5 wt % organoclay [Fig. 7(A,C,E,G)], the space between layered silicates was about 5–10 nm, and a larger portion of silicates became exfoliated, especially for the PU/3K-M-3K nanocomposite, in comparison with the nanocomposites containing 3 wt % organoclay. On the basis of the aforementioned SEM and TEM results, it was confirmed that the layered silicates were easily exfoliated when the organoclay content in the polymer matrix was lower (0.5 wt %), whereas a mostly intercalated structure of layered silicates and some aggregation of clay particles in the matrix were observed when the clay loading increased to 3 wt %. The average *d*-spacing of the PU/clay nanocomposites from TEM images is shown in Figure 8. The nanocomposites containing organifiers of higher molecular weights showed wider *d*-spacing in the same series (PU/2K-M-2K < PU/3K-M-3K, PU/2K-

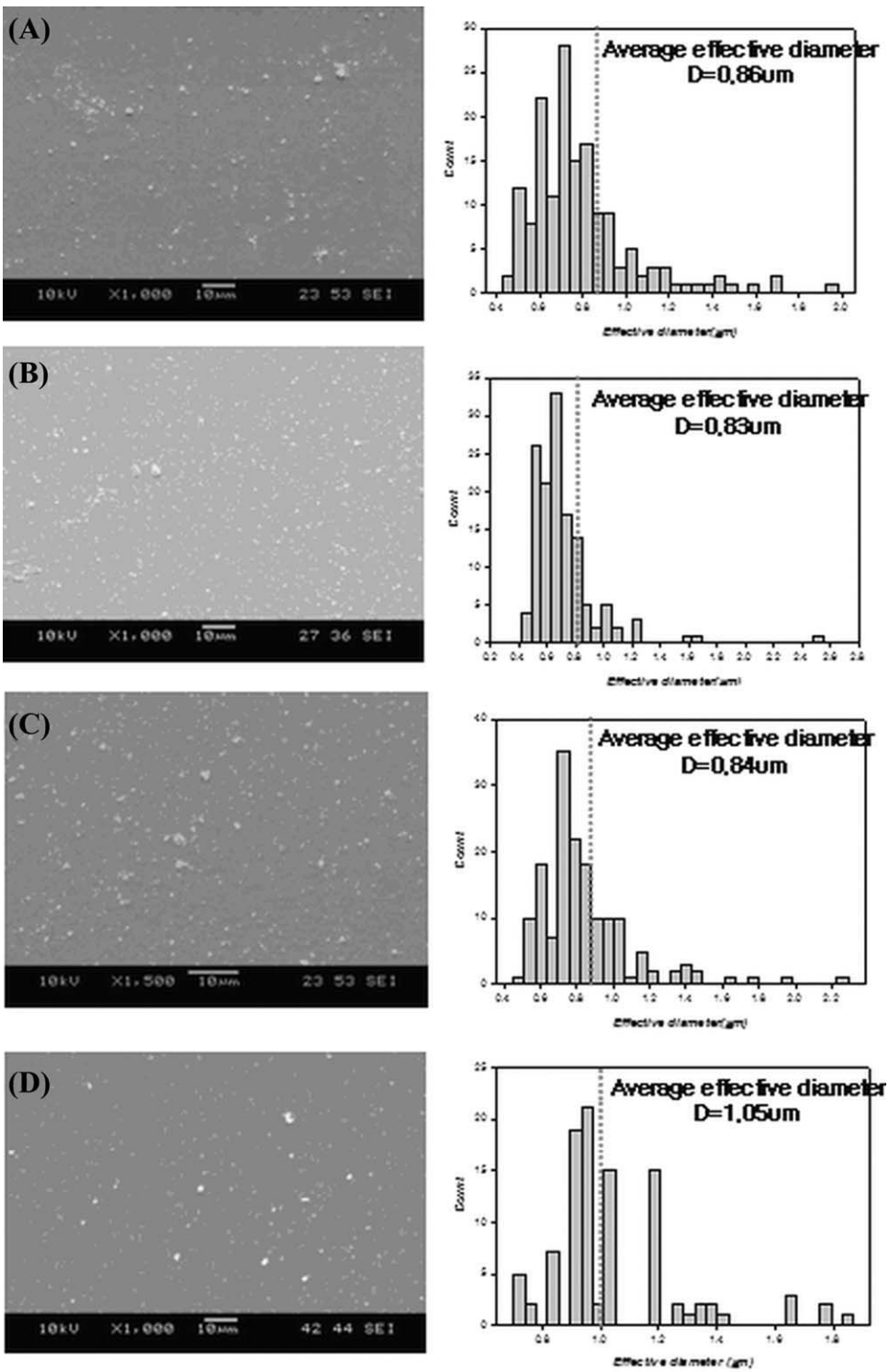

Figure 4 SEM micrographs of spin-coated organoclays after sonication in DMF for 10 min: (A) 2K-M-2K, (B) 3K-M-3K, (C) 2K-M-1K-M-2K, and (D) 2K-M-3K-M-2K.

M-1K-M-2K < PU/2K-M-3K-M-2K), and the nanocomposites with the one-binding-site organoclay demonstrated better penetration of PU into the silicate layers because more organifier was replaced by the Na cation during the cation-exchange reaction.

Molecular weight

The molecular weights of the neat PU and PU/clay nanocomposites are listed in Table II. Neat PU had a number-average molecular weight of 80,000 and a weight-average molecular weight of 150,000. The

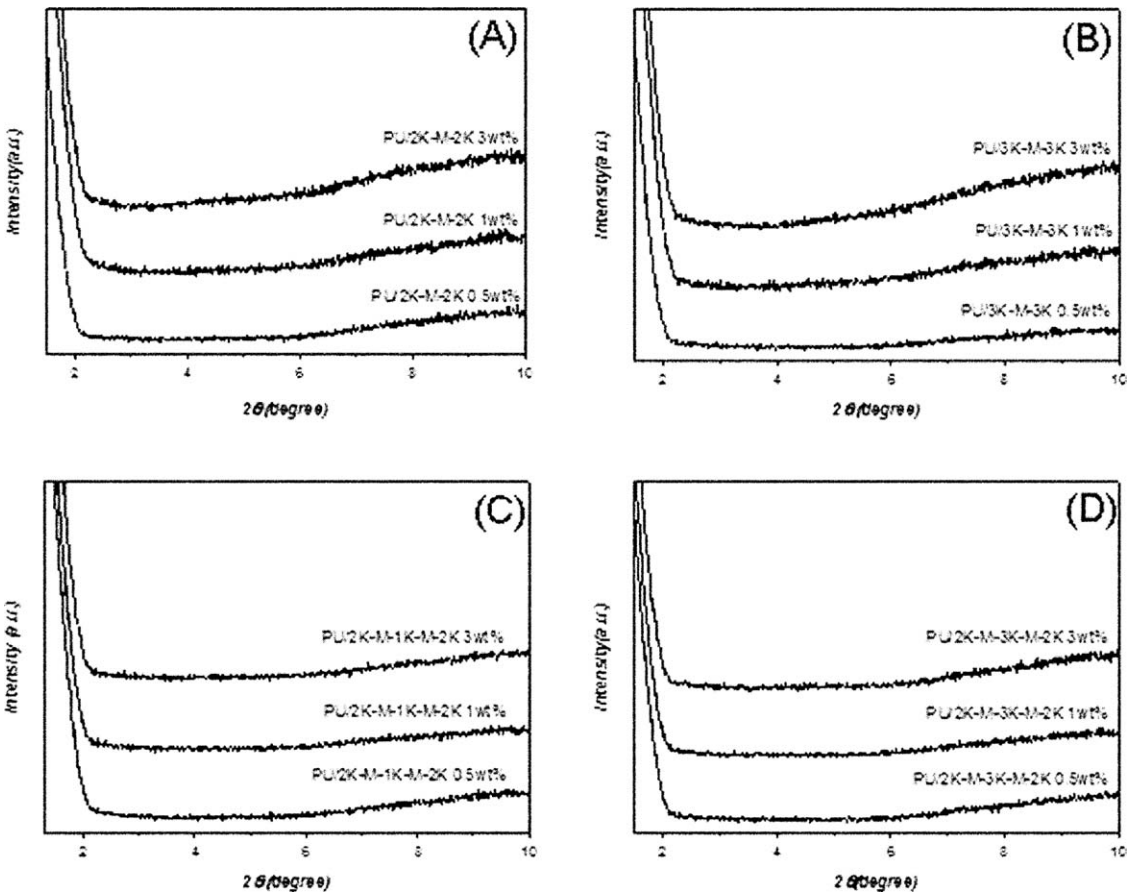

Figure 5 WAXD patterns of PU/clay nanocomposites with different organoclay loadings: (A) PU/2K-M-2K, (B) PU/3K-M-3K, (C) PU/2K-M-1K-M-2K, and (D) PU/2K-M-3K-M-2K.

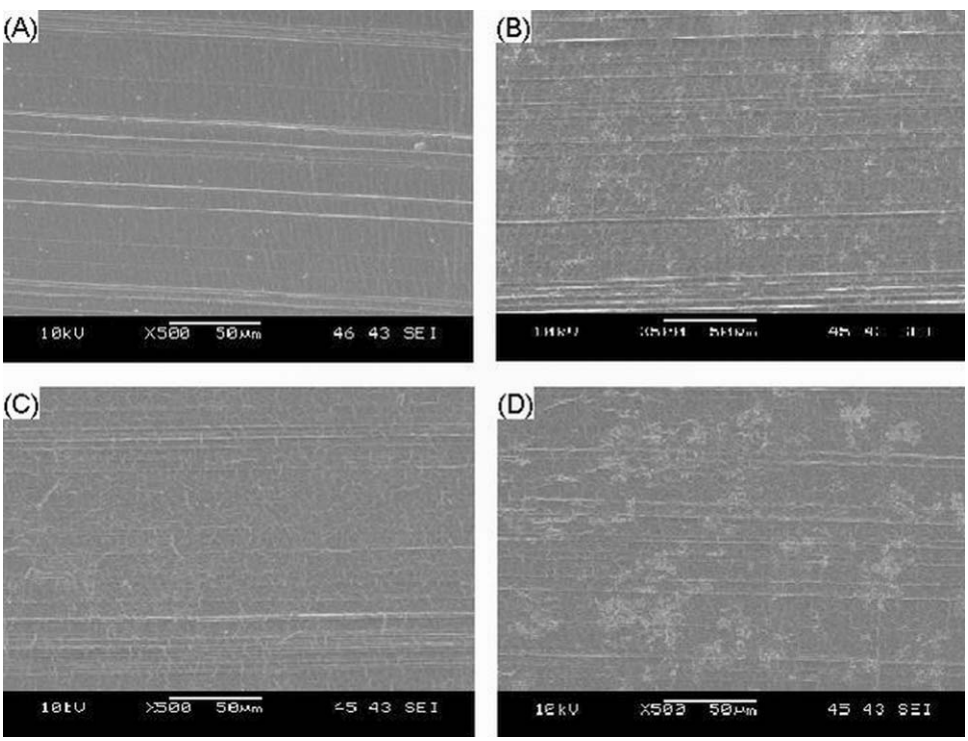

Figure 6 SEM images of PU/clay nanocomposites with various organoclay loadings: (A) PU/2K-M-2K (0.5 wt %), (B) PU/2K-M-2K (3 wt %), (C) PU/2K-M-1K-M-2K (0.5 wt %), and (D) PU/2K-M-1K-M-2K (3 wt %).

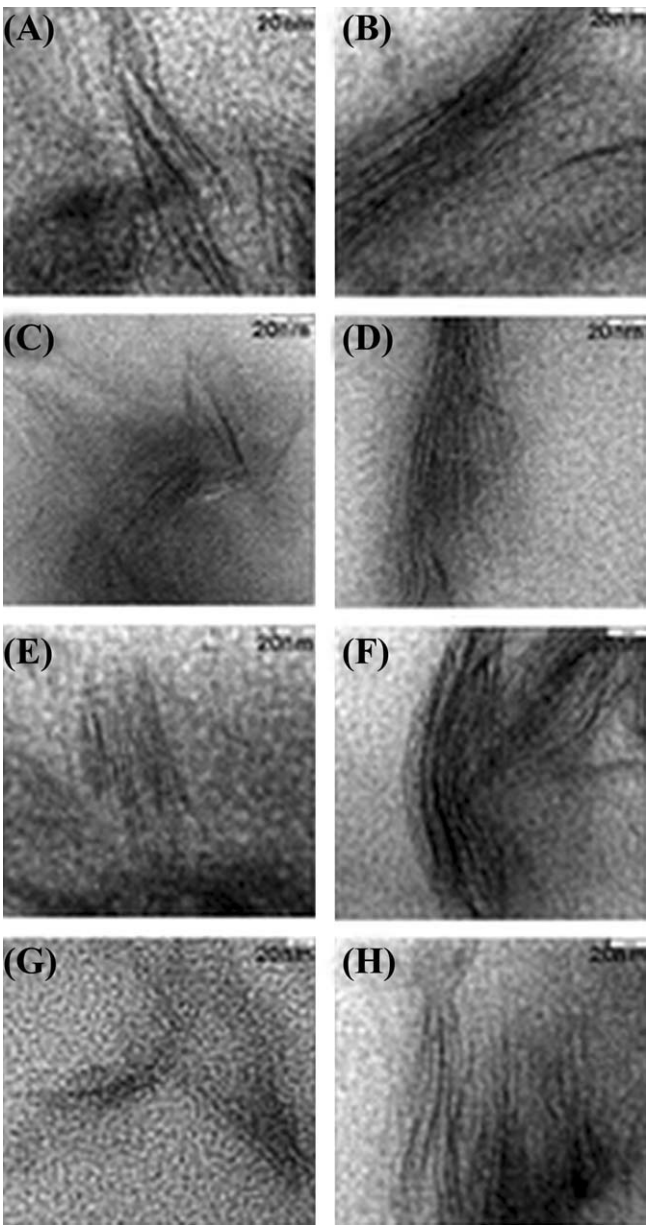

Figure 7 TEM images of PU/clay nanocomposites with various organoclay loadings: (A) PU/2K-M-2K (0.5 wt %), (B) PU/2K-M-2K (3 wt %), (C) PU/3K-M-3K (0.5 wt %), (D) PU/3K-M-3K (3 wt %), (E) PU/2K-M-1K-M-2K (0.5 wt %), (F) PU/2K-M-1K-M-2K (3 wt %), (G) PU/2K-M-3K-M-2K (0.5 wt %), and (H) PU/2K-M-3K-M-2K (3 wt %).

number-average molecular weight of the nanocomposites increased in comparison with the neat PU and also increased with the clay content increasing from 0.5 to 3 wt %. The hydroxyl end groups of the organifier could react with isocyanates during polymerization, so the organifier could act as a chain extender. By sonication, clay aggregates could be broken into fine clay particles, and more organifier could be exposed to the reaction medium during polymerization. Therefore, nanocomposites with a higher clay content (3 wt %) showed slightly higher molecular weights than nanocomposites of a lower clay content (0.5 wt %).

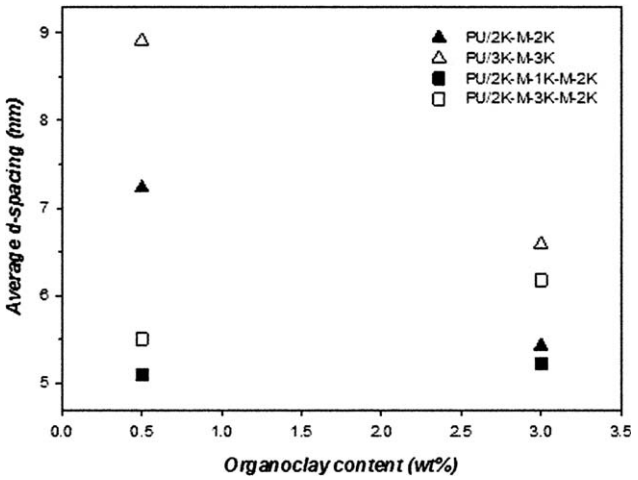

Figure 8 Average *d*-spacings of PU/clay nanocomposites with 0.5 or 3 wt % organoclay loadings (from TEM images).

Thermal properties

Glass-transition temperature

The peak of the tan δ curve from DMTA was determined as the glass-transition temperature. The glass-transition temperatures of the soft segment of the neat PU and PU/clay nanocomposites are listed in Table III. The glass-transition temperature (T_g) of the nanocomposites was higher than that of the neat PU on account of the physical crosslinking generated through the ionic bonding between the PU chain and the silicate surface because the hydroxyl end group of the organifier could react with the

TABLE II
Molecular Weights and Molecular Weight Distributions of the Neat PU and PU/Clay Nanocomposites

Sample	Clay content (wt %)	M_n	M_w	PDI
Neat PU	0	80,000	150,000	1.94
PU/2K-M-2K	0.5 (0.16)	101,000	191,000	1.90
	1 (0.32)	126,000	251,000	1.86
	3 (0.96)	142,000	240,000	1.69
PU/3K-M-3K	0.5 (0.12)	98,000	192,000	1.95
	1 (0.24)	114,000	223,000	1.96
	3 (0.72)	122,000	229,000	1.87
PU/2K-M-1K-M-2K	0.5 (0.22)	93,000	196,000	2.00
	1 (0.44)	109,000	208,000	1.90
	3 (1.32)	112,000	230,000	1.90
PU/2K-M-3K-M-2K	0.5 (0.16)	97,000	186,000	1.91
	1 (0.32)	110,000	194,000	1.75
	3 (0.97)	114,000	212,000	1.86

M_n = number-average molecular weight; M_w = weight-average molecular weight; PDI = polydispersity index.

TABLE III
Thermal Properties of the Neat PU and PU/Clay Nanocomposites

Sample	Clay content (wt %)	T_g (°C)	T_{OD} (°C)	$T_{max,1}$ (°C)	$T_{max,2}$ (°C)
Neat PU	0	−20.2	237.8	317.7	386.0
PU/2K-M-2K	0.5 (0.16)	−15.7	279.3	346.1	439.8
	1 (0.32)	−13.1	281.2	347.4	443.1
	3 (0.96)	−12.4	282.5	353.0	443.4
PU/3K-M-3K	0.5 (0.12)	−14.6	280.6	339.0	440.0
	1 (0.24)	−12.3	282.3	347.9	441.1
	3 (0.72)	−11.5	283.6	350.6	449.1
PU/2K-M-1K-M-2K	0.5 (0.22)	−15.6	276.7	345.9	442.1
	1 (0.44)	−13.1	280.3	347.9	445.3
	3 (1.32)	−12.1	282.5	356.1	460.8
PU/2K-M-3K-M-2K	0.5 (0.16)	−13.3	279.5	346.8	443.2
	1 (0.32)	−12.4	280.7	350.5	444.6
	3 (0.97)	−11.7	281.8	355.7	445.0

T_g = glass-transition temperature; $T_{max,1}$ = temperature of the maximum decomposition rate for the first stage; $T_{max,2}$ = temperature of the maximum decomposition rate for the second stage; T_{OD} = onset degradation temperature.

isocyanate group during the polymerization. The other cause for the increase in the glass-transition temperature with the addition of the organoclay was the confinement effect of the segmental motions of intermolecular chains of the polymer within the clay galleries.[42] With the clay content increasing from 0.5 to 3 wt %, the glass-transition temperatures of the nanocomposites also increased, and the glass-transition temperature was shifted about 8°C when 3 wt % clay was added. Additionally, nanocomposites containing a higher molecular weight organifier showed a higher glass-transition temperature in the same series (PU/2K-M-2K and PU/3K-M-3K, PU/2K-M-1K-M-2K, and PU/2K-M-3K-M-2K) because of the better dispersibility of the organoclays in the PU matrix, and this resulted in a stronger interaction between the PU matrix and clay.

Thermal stability

It is generally believed that the introduction of an inorganic component into organic materials can improve their thermal stability because the inorganic component possesses good thermal stability. Thermogravimetric analysis results for the neat PU and PU/clay nanocomposites are summarized in Table III. The thermal degradation of PU occurred in two stages: the first stage was mainly governed by the degradation of the hard segment, and the second stage correlated well with the degradation of the soft segment.[3] The onset temperature of degradation and the temperatures of the maximum decomposition rate for the first and second stages were determined. With the addition of the organoclay, the thermal stability of the nanocomposites was significantly increased in comparison with the neat PU. As listed in Table III, the thermal stability of the nanocomposites at the onset degradation temperature (T_{OD}) and the temperatures of the maximum decomposition rate for the first ($T_{max,1}$) and second stages ($T_{max,2}$) was about 46, 38, and 75°C higher than that of the neat PU at the maximum, respectively. The enhanced thermal stability through the introduction of organoclays into the polymer matrix could be attributed to the dispersed clay particles, which acted as a mass transport barrier, hindering the permeability of volatile degradation products out of the materials.[3]

Tensile properties

The tensile strength, elongation at break, and Young's modulus of the neat PU and PU/clay nanocomposites are shown in Figure 9 and summarized in Table IV. It is well known that a nanodispersed

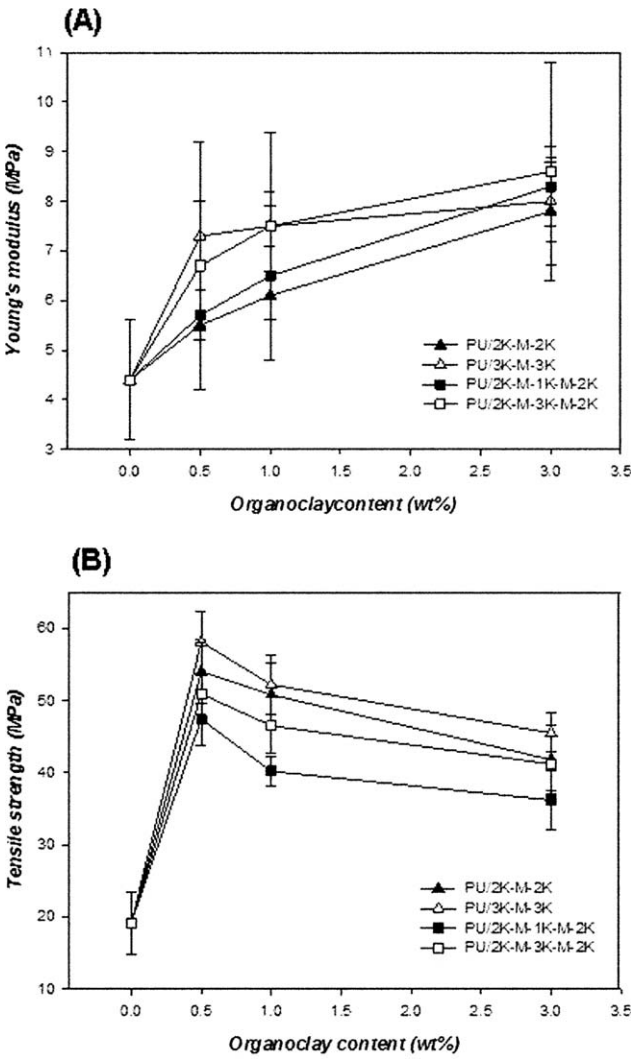

Figure 9 Variations of (A) Young's modulus and (B) the tensile strength of PU/clay nanocomposites with different organoclay loadings.

TABLE IV
Summary of the Tensile Properties

Sample	Clay content (wt %)	Young's modulus (MPa)	Tensile strength (MPa)	Elongation at break (%)
Neat PU	0	4.4 ± 1.2	19.2 ± 4.3	879 ± 50
PU/2K-M-2K	0.5 (0.16)	5.5 ± 1.3	54.0 ± 4.5	882 ± 56
	1 (0.32)	6.1 ± 0.5	50.8 ± 4.4	774 ± 78
	3 (0.96)	7.8 ± 1.1	41.8 ± 4.8	735 ±87
PU/3K-M-3K	0.5 (0.12)	7.3 ± 1.9	58.1 ± 4.3	787 ± 85
	1 (0.24)	7.5 ± 0.4	52.2 ± 4.1	778 ± 40
	3 (0.72)	8.0 ± 0.8	45.5 ± 2.7	708 ± 22
PU/2K-M-1K -M-2K	0.5 (0.22)	5.7 ± 0.5	47.4 ± 3.6	684 ± 46
	1 (0.44)	6.5 ± 1.7	40.2 ± 2.0	654 ± 52
	3 (1.32)	8.3 ± 0.8	36.2 ± 4.2	619 ± 41
PU/2K-M-3K -M-2K	0.5 (0.16)	6.7 ± 1.3	50.9 ± 7.1	765 ± 89
	1 (0.32)	7.5 ± 1.9	46.5 ± 3.9	669 ± 87
	3 (0.97)	8.6 ± 2.2	41.2 ± 3.8	614 ± 88

clay with a high aspect ratio reduces the molecular mobility of polymer chains, resulting in a less flexible material with a higher Young's modulus.[32] Therefore, Young's modulus increases with the clay content and the dispersibility of the organoclay increasing.[3] As shown in Figure 9(A), Young's modulus increased with the clay content increasing, and Young's modulus increased by about 49% for the PU/2K-M-3K-M-2K nanocomposite in comparison with that for the neat PU.

It is believed that the strong ionic bonding between the quaternary ammonium cation in the PU main chain and the oxygen anion on the surface of the silicate layer[3] increased the tensile strength of the nanocomposites. As a result, the tensile strength increased with the introduction of the organoclays into the PU matrix and showed a maximum value with a 0.5 wt % clay loading (a 200% increase in the tensile strength for PU/3K-M-3K). However, with the clay content increasing from 0.5 to 3 wt %, a decrease in the tensile strength was observed for all the nanocomposites. The reason was mainly the agglomeration of organoclays in the PU matrix, as discovered in the SEM and TEM investigations. Because of the agglomeration of the clay particles, the layer–layer interaction was predominant over the layer–polymer interaction, and the agglomerated particles acted as defects. In addition, nanocomposites containing organifiers of higher molecular weights had higher tensile strength in the same series because of the better dispersibility of the organoclays in the PU matrix.

CONCLUSIONS

A reactive organifier with tertiary amine and hydroxyl end groups was successfully synthesized, and pristine Na-MMT was treated with the organifier. PU/clay nanocomposites were synthesized to investigate the effect of ionic crosslinking by the introduction of multiple cationic sites with organifiers of different molecular weights. A better dispersion of the organoclay in the PU matrix was achieved by the application of sonication to a suspension of the organoclay in DMF, and the average size of the organoclay was reduced to about 1 μm. The *d*-spacing of the organoclay (2K-M-1K-M-2K) was found to be 1.97 nm versus 1.13 nm for Na-MMT, and the peak intensity decreased with the molecular weight of the organifier increasing in the same series (2K-M-2K and 3K-M-3K, 2K-M-1K-M-2K and 2K-M-3K-M-2K). However, no peaks were detected in WAXD patterns for the PU/clay nanocomposites because the amount of clay was too small to be detected. Because XRD could detect only the periodic stacked *d*-spacing of samples, TEM was used to determine the nanoscale morphology of the nanocomposites. Both intercalated and exfoliated structures were found in the TEM images, and the *d*-spacing ranged from 4 to 10 nm. A small amount of the organoclay in the PU matrix could obviously improve the thermal and mechanical properties because of the strong interaction between the PU matrix and the organoclay. The onset degradation temperature of the nanocomposites increased by about 40–46°C with respect to that of neat PU; the maximum values of Young's modulus and the tensile strength of the nanocomposites also increased by about 49 and 200% in comparison with neat PU. The tensile strength showed a maximum with a 0.5 wt % organoclay loading and decreased with the clay content increasing because of the agglomeration of the organoclay. The glass-transition temperature and mechanical properties of the nanocomposites containing a higher molecular weight organifier showed higher values in the same series because of the better dispersibility of the organoclay. Unfortunately, the effect of multi-binding-site organifiers on the properties of the nanocomposites was not as significant as the molecular weight because Na cations on the silicate surface were not replaced enough by the organifiers (ion-exchanged fraction = 0.24 for the 2K-M-1K-M-2K organoclay).

References

1. Pinnavaia, T. J.; Beall, G. Polymer–Clay Nanocomposites; Wiley: Chichester, England, 2000.
2. Kojima, Y.; Usuki, A.; Kawasumi, M.; Okada, A.; Fukushima, Y.; Kurauchi, T.; Kamigaito, O. J Mater Res 1993, 8, 1185.
3. Choi, W. J.; Kim, S. H.; Kim, Y. J.; Kim, S. C. Polymer 2004, 45, 6045.
4. Usuki, A.; Kawasumi, M.; Kojima, Y.; Kurauchi, T.; Kamigaito, O. J Mater Res 1993, 8, 1174.
5. Usuki, A.; Kojima, Y.; Kawasumi, M.; Okada, A.; Fukushima, Y.; Kurauchi, T.; Kamigaito, O. J Mater Res 1993, 8, 1179.

6. Kojima, Y.; Usuki, A.; Kawasumi, M.; Okada, A.; Kurauchi, T.; Kamigaito, O. J Polym Sci Part A: Polym Chem 1993, 31, 1755.
7. Lepoittevin, B.; Devalckenaere, M.; Pantoustier, N.; Alexandre, M.; Kubies, D.; Calberg, C.; Jerome, R.; Dubois, P. Polymer 2002, 43, 4017.
8. Chavarria, F.; Nairn, K.; White, P.; Hill, A. J.; Hunter, D. L.; Paul, D. R. J Appl Polym Sci 2007, 105, 2910.
9. Gilman, J. W.; Jackson, C. L.; Morgan, A. B.; Harris, R.; Manias, E.; Gianellis, E. P.; Wuthenow, M.; Hilton, D.; Philips, S. H. Chem Mater 2000, 12, 1866.
10. Ghosh, A. K.; Woo, E. M. Polymer 2004, 45, 4749.
11. Chigwada, G.; Wang, D.; Jiang, D. D.; Wilkie, C. A. Polym Degrad Stab 2006, 91, 755.
12. Agag, T.; Koga, T.; Takeichi, T. Polymer 2001, 42, 3399.
13. Campbell, S.; Liang, M. I. High Perform Polym 2006, 18, 71.
14. Ema, Y.; Ikeya, M.; Okamoto, M. Polymer 2006, 47, 5350.
15. Xu, W.; Raychowdhury, S.; Jiang, D. D.; Retsos, H.; Giannelis, E. P. Small 2008, 4, 662.
16. Tjong, S. C.; Meng, Y. Z. J Polym Sci Part B: Polym Phys 2003, 41, 2332.
17. Wang, K.; Liang, S.; Du, R.; Zhang, Q.; Fu, Q. Polymer 2004, 45, 7953.
18. Deenadayalan, E.; Vidhate, S.; Lele, A. Polym Int 2006, 55, 1270.
19. Shah, D.; Maiti, P.; Gunn, E.; Schmidt, D. F.; Jiang, D. D.; Batt, C. A.; Giannelis, E. P. Adv Mater 2004, 16, 1173.
20. Park, J. H.; Jana, S. C. Polymer 2003, 44, 2091.
21. Cui, L.; Tarte, N. H.; Woo, S. I. Macromolecules 2008, 41, 4268.
22. Chang, C. C.; Hou, S. S. Eur Polym J 2008, 44, 1337.
23. Wang, Z.; Pinnavaia, T. J. Chem Mater 1998, 10, 1820.
24. Maji, P. K.; Guchhait, P. K.; Bhowmick, A. K. Appl Mater Interfaces 2009, 1, 289.
25. Chen-Yang, Y. W.; Yang, H. C.; Li, G. J.; Li, Y. K. J Polym Res 2004, 11, 275.
26. Chen-Yang, Y. W.; Lee, Y. K.; Chen, Y. T.; Wu, J. C. Polymer 2007, 48, 2969.
27. Rehab, A.; Salahuddin, N. Mater Sci Eng A 2005, 399, 368.
28. Xiong, J.; Liu, Y.; Yang, X.; Wang, X. Polym Degrad Stab 2004, 86, 549.
29. Xiong, J.; Zheng, Z.; Jiang, H.; Ye, S.; Wang, X. Compos A 2007, 38, 132.
30. Ni, P.; Wang, Q.; Li, J.; Suo, J.; Li, S. J Appl Polym Sci 2006, 99, 6.
31. Chen, T. K.; Tie, T. I.; Wei, K. H. Polymer 2000, 41, 1345.
32. Uhl, F. M.; Davuluri, S. P.; Wong, S. C.; Webster, D. C. Polymer 2004, 45, 6175.
33. Subramani, S.; Choi, S. W.; Lee, J. Y.; Kim, J. H. Polymer 2007, 48, 4691.
34. Cao, F.; Jana, S. C. Polymer 2007, 48, 3790.
35. Chavarria, F.; Paul, D. R. Polymer 2006, 47, 7760.
36. Zheng, J.; Ozisik, R.; Siegel, R. W. Polymer 2006, 47, 7786.
37. Dan, C. H.; Lee, M. H.; Kim, Y. D.; Min, B. H.; Kim, J. H. Polymer 2006, 47, 6718.
38. Meng, X.; Du, X.; Wang, Z.; Bi, W.; Tang, T. Compos Sci Technol 2008, 68, 1815.
39. Chen, H.; Zheng, M.; Sun, H.; Jia, Q. Mater Sci Eng A 2007, 445, 725.
40. Tien, Y. I.; Wei, K. H. Macromolecules 2001, 34, 9045.
41. Korley, L. T. J.; Liff, S. M.; Kumar, N.; McKinley, G. H.; Hammond, P. T. Macromolecules 2006, 39, 7030.
42. Dai, X.; Xu, J.; Guo, X.; Lu, Y.; Shen, D.; Zhao, N.; Luo, X.; Zhang, X. Macromolecules 2003, 37, 5615.
43. Mishra, J. K.; Kim, I.; Ha, C. S. Macromol Rapid Commun 2003, 24, 671.
44. Kim, D. S.; Kim, J. T.; Woo, W. B. J Appl Polym Sci 2005, 96, 1641.
45. Paul, D. R.; Robeson, L. M. Polymer 2008, 49, 3178.
46. Lee, H. T.; Lin, L. H. Macromolecules 2006, 39, 6133.
47. Hepbum, C. Polyurethane Elastomers, 2nd ed.; Elsevier Science: Essex, England, 1992; Chapter 11, p 280.